9

Planetary Structures and Tectonics

The surfaces of terrestrial planets and icy satellites have enjoyed deformation marked by faults and folds. We use these geologic structures not only to characterize the morphology of the surfaces, but also to describe the motions, stresses, and deformation processes that created the structures. Ultimately, we can sum these structural data and interpretations to infer the tectonic deformation for large portions of, or even entire, planets and satellites. As we will see, understanding deformation at this large tectonic scale enables us to investigate what is driving overall planet or satellite development. We will also learn that while the expected will happen, conundrums exist too. For example, the rocks of terrestrial planets deform quite differently from the icy shells of the satellites of the gas giants, yet the magnitude of these differences and their causes can surprise us. On the other hand, Venus and Earth are quite similar in many planetary characteristics but have strikingly different tectonic histories, which challenges us to understand why.

9.1 Active-Lid versus Stagnant-Lid Planets and Satellites

If the lithospheres of planets and satellites were continuous and attached to underlying mantles and cores, this chapter would likely be a short description of structures related to long-term cooling shrinkage of the bodies and impact cratering. Such bodies with immobile and intact **stagnant lids** are abundant in the Solar System (Figure 9.1a). Yet, we also have bodies with **active lids**, such as the Earth and Europa, with lithospheres that are able to develop faults/shear zones and deform significantly in response to driving stresses related to agents such as mantle convection or eccentric orbits. In between, we have bodies such as Mars, which through much of its history has been stagnant lid, but with greater tectonic deformation than expected due to Tharsis, or Venus, which is presently stagnant lid, but has evidence to indicate that possibly it was episodically an active lid in the past.

Considering planets and satellites from the perspective of structural geology and tectonics, the contrast between stagnant and active lids is fundamental. For example, a stagnant-lid body such as Mercury dominantly shrank through its history due to cooling, so that contractional structures on its surface record a very modest shortening strain. In contrast, the active-lid Earth has individual thrust faults in single mountain belts that each accommodated displacements that are 2–5 times greater than the total shortening recorded for Mercury. Consequently, active-lid and possibly episodically active-lid bodies display a much richer abundance and range of tectonic structures representing more complex histories than found for stagnant-lid bodies (Figure 9.1b).

Given the range of behaviors from simple stagnant-lid to fully active-lid bodies in the Solar System, understanding what controls the occurrence of particular behaviors is essential to grasping their tectonic development. A necessary requirement for active-lid behavior is that the driving stress from the agent powering the deformation exceeds lithospheric strength (see Chapter 8 for quantitative consideration of the driving stresses and onset of deformation). For example, if the agent is mantle convection, then the stresses generated by mantle circulation are sufficient to cause breakage of the overlying lithosphere so that segments of the lid can move relative to each other, creating active-lid behavior (O'Neill et al., 2007).

Additionally for the case of mantle convection, the thermal and deformation history can play a role in whether active- or stagnant-lid behavior is present. For example, transitioning from stagnant lid to active lid is more difficult than from active to stagnant for two reasons. First, stagnant lids tend to be thicker than active

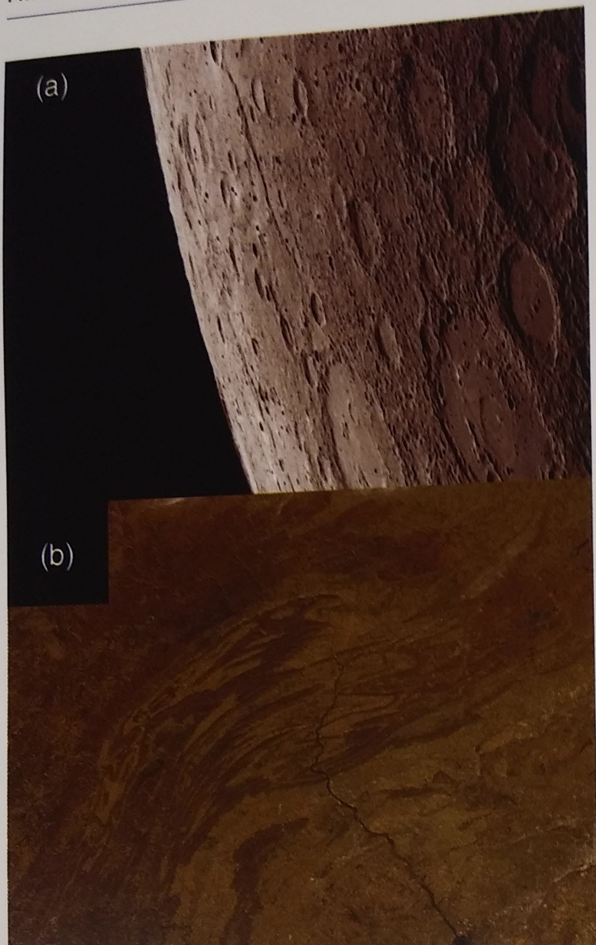

Figure 9.1 (a) Surface image of Mercury, which experienced stagnant-lid tectonics. Abundant craters of various sizes accumulated over time and very few topographic features are related to faults or folds. This image does contain a prominent north–south trending tectonic lobate ridge in its middle. Image from *MESSENGER*. (b) Image of a planetary surface that experienced active-lid tectonics. Portion of the Appalachian mountain belt in North America that formed due to collision between two lid segments, creating abundant faults and folds. NASA *Aqua Satellite* image.

lids, with greater vertical thermally inefficient, conductive cooling paths, so heat is trapped in the underlying mantle, reducing its viscosity (strength) (Weller and Lenardic, 2012). Second, the thicker stagnant lid will have greater yield strength, as we will see in the next section about lithospheric material properties, which reduces the ability of mantle convection to trigger lithospheric failure.

9.2 Lithospheric Materials, Deformation Behaviors, and Strengths

While a number of factors influence the occurrence of active- versus stagnant-lid behavior, the crux of the matter is the interplay of the magnitudes of the driving forces from causative agents versus the lithospheric material strength.

9.2.1 Materials

The compositions of planetary and satellite lithospheres are critical to determining their material strengths. As we are focusing on terrestrial planets and the Moon, and on icy satellites of the gas giants, we are dealing with lithospheres composed of rock or ice, respectively. While these materials can be quite complex as a function of being polymineralic, having different grain sizes and containing a variety of impurities or fluids, we will keep our considerations simple, so as to focus on the major aspects of their deformation behaviors.

For most rocky bodies, we are dealing with exterior mafic igneous rocks (basalt, gabbro) and internal ultramafic rocks (peridotite) in the lithosphere to a first order, so the suite of minerals commonly includes a primary mix of olivine, pyroxene, amphibole, plagioclase, and garnet. Ideally, we would construct our material understanding from these rocks using their mineral suites allowing for compositional variation, grain size variation, etc. At this time, our experimental and simulation capabilities for rocks limit our ability to characterize and usefully predict the deformation behavior of these natural materials. So, we will use a single mineral that is common to these rocks to serve as a proxy for their behavior: olivine, the ferromagnesian silicate containing a structure of isolated silica tetrahedra with orthorhombic symmetry. The robustness of using this proxy is based on over 50 years of actual deformation experiments and 25 years of computer-simulated deformation including polycrystalline aggregates interpreted in terms of comparisons to naturally deformed rocks from Earth.

For icy satellites, we are restricted to information about their exteriors for nominating a proxy of their deformation behavior. Almost all exteriors have ice compositions dominated by water although methane or ammonia may be in the mix. Thus, water ice serves as our proxy, and in particular Phase I water ice (henceforth, just water ice). Other phases of ice typically require confining pressures that would place their occurrence at several hundred kilometers depth within satellites, and the consensus is that the ice/water layer for these bodies does not normally reach that thickness for the satellites with visible tectonic deformation. An important limitation is that useful ice deformation experiments and simulations are much fewer than for rocks and only date back about 30 years. Further, we lack naturally deformed ice samples from the satellites, and ice from Earth's glaciers and ice sheets deforms at much higher temperatures than found on the satellite exteriors. So, our understanding of material behavior for ice-bearing lithospheres is more speculative than for rock-bearing lithospheres.

9.2.2 Deformation Behaviors

Materials deform in three basic ways: elastically, brittlely, or ductilely. During an elastic deformation when the causative stress state is relaxed, the material returns to its original condition and the deformation is recoverable (further explained in Section 8.2). By contrast, brittle and ductile deformations are permanent and not recovered when the causative stress state is relaxed. For brittle deformation, the material breaks and grain attrition processes such as wear and fracture occur to accommodate displacement, whereas for ductile deformation the material flows without breakage. Two end member types of flow are viscous deformation where the flow rate is a function of the differential stress magnitude, and plastic deformation where flow does not occur until reaching a threshold or yield stress.

Olivine and water ice display combinations of these behaviors during deformation. For example, in the upper lithosphere where temperatures and pressures are lower, small deformations are typically elastic and larger and/or faster deformations are brittle. Likewise, very small deformations are elastic and larger/faster ones are permanent in the lower lithosphere. In this case, the permanent deformation will be the interplay of viscous flow often related to deformation processes involving atomic diffusion (creep processes) and plastic flow related to overcoming yield strengths for glide systems within atomic lattices (dislocation glide) or on grain boundaries (grain-boundary sliding).

An important point to consider when comparing the behaviors of ice-bearing and rock-bearing lithospheres is whether olivine and water ice are similar or different as deforming materials. Elastically, they differ as the stiffness (Young's modulus) of olivine is about 50 GPa, whereas in water ice it is about 9 GPa, so olivine is a much stronger elastic material than ice. Frictionally, they are quite similar initially in that both have coefficients of friction, which is the resistance to sliding on a surface, of about 0.45 to 0.55. So, once sliding surfaces form, both materials display similar resistance to slip. Ductilely, olivine and water ice are again quite different. Ice has a much lower melting temperature and therefore at much lesser depths in a lithosphere nears its melting temperature, unlike olivine. In fact, for olivine and considering the Earth, a current debate is whether the base of oceanic lithosphere at the asthenosphere is due to a small amount of melting or melting is unneeded because thermally driven deformation has become very efficient (e.g., Boettcher et al., 2007; Hansen et al., 2016). So, the olivine-rich oceanic lithosphere of the Earth may not reach its melting temperature at any depth, making it stronger when compared to ice! Further, as water ice is 10^4–10^8 times less viscous than olivine, ice flows much more easily for the same driving stress and is thus much weaker as a ductile material. In summary, water ice with respect to olivine is weaker elastically and easier to break, similarly strong initially as a brittle sliding material, and much weaker as a ductile material due to a lower melting temperature and lesser viscosity. Simply, water ice is more susceptible to deformation than olivine (rock), and we will see the implications of this difference when we consider Europa.

9.2.3 Lithospheric Strength as a Function of Depth

Given knowledge of our materials and their deformation behaviors, we can identify the depth at which the lithosphere is strongest, which is where the driving stress must be greatest to trigger active-lid tectonics. Assuming a compositionally homogeneous lithosphere with a constant grain size for simplicity, we first consider the Earth as a representative for rocky bodies. The strength of the lithosphere is a function of depth, where depth serves as a proxy for temperature and confining pressure (Figure 9.2a). In a stressed material, different deformation behaviors compete as a function of conditions such as pressure, differential or shear stress, and confining temperature, and the most efficient behaviors tend to dominate, setting the local value for lithospheric strength. Overall, in the lithosphere, this competition is between brittle frictional versus ductile viscous and/or plastic processes. The frictional processes require shear stresses to exceed the coefficient of friction and the normal stress, which is a function of overburden and the tectonic stresses. The viscous and plastic processes that are inversely and nonlinearly related to temperature and hence, the reservoir of heat energy, require sufficient differential stresses to drive deformation processes such as atomic diffusion, lattice sliding, grain-boundary sliding, grain-boundary nucleation, and grain-boundary migration. Consequently, the cooler upper lithosphere is dominantly elastofrictional, whereas much of the lower hotter lithosphere deforms viscously and/or plastically. The depth at which the lithosphere transitions from elastofrictional to viscous/plastic is the **Brittle–Ductile Transition** (BDT in Figure 9.2). This depth is also the position of the greatest strength in the lithosphere because it has the greatest normal stress on a potential translithospheric fault for the brittle regime, and the least available amount of heat energy for deformation in the ductile regime.

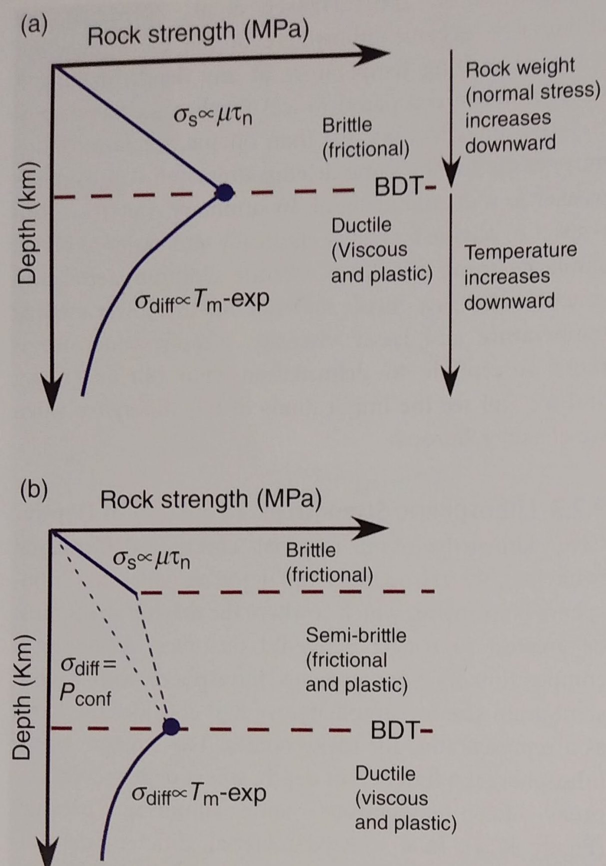

Figure 9.2 (a) Graph of depth versus rock strength for (a) idealized olivine lithosphere, and (b) idealized olivine lithosphere where brittle and plastic deformation mechanisms are both active above the Brittle–Ductile Transition (BDT). Large blue dot marks the depth of greatest rock strength, where normal stress is greatest in the brittle regime and temperature is lowest in the ductile regime. σ_s is shear stress, μ is coefficient of friction, σ_n is normal stress, σ_{diff} is differential stress, T_m is melting temperature, τ_n and P_{conf} is confining pressure.

Ice lithospheres may differ from olivine-dominated lithospheres by having an elastic zone between the brittle and ductile lithospheric regimes, if driving stresses are insufficient for brittle failure in the lower elasto-plastic lithosphere. Another variation of lithospheric strength with depth occurs with olivine due to the competition of deformation mechanisms above the ductile regime. There, both frictional and dislocation-related plastic processes may be occurring with near equal efficiency in the rock so that the lithosphere has a composite semi-brittle behavior (Figure 9.2b). Yet, in any of these cases, the top of the ductile regime is the strongest position in the lithosphere and that is the strength value that must be exceeded by driving stresses for active-lid tectonics to initiate.

9.3 Energy Sources and Driving Stresses

Tectonic deformation requires energy, which can be derived from a variety of sources. These include response to temperature changes, unstable density configurations, tidal distortions and, on icy bodies, true polar wander.

9.3.1 Thermal Sources

Temperature and, more importantly, cooling and heating, have quite opposite roles as an energy source for driving tectonic deformation. The long-term cooling of a planet or satellite results from the body releasing heat to the cold of space. If the body is not generating sufficient replacement heat through processes such as radioactive decay, buoyancy effects with potential energy releases or major impacts, it cools. Within the body, heat release is a combination of outward heat conduction and convection that leads to thermal contraction of solids, solidification of liquids, and phase changes to denser minerals (see Sections 8.5 and 8.6 for further explanation). These processes typically are operating over most of the history of a body, excluding the early heavy bombardment period, up to the present day. The primary physical effect of this cooling is a reduction in the radius of the planet or satellite. As the surface area of such a body is dependent on its radius, a radial reduction requires an areal reduction triggering horizontally directed, contractional tectonic deformation on the surface of a body. As we will see, Mercury is an excellent example of this phenomenon.

The other role relates more to heat flow than heat release and for terrestrial bodies concerns the vigor of mantle convection and its ability to affect lithospheric behavior and deformation. We know from our consideration of material strength for the lithosphere that mantle convection initiates active-lid tectonics by creating sufficient stress to overcome the lithospheric strength at the BDT. Consequently, the velocity of mantle convection and the viscosity of the convecting mantle are key to determining whether convection generates sufficient stress to trigger failure. Another important attribute is the degree of traction between the base of the lithosphere and the underlying mantle, which is assumed to be strong even if an asthenosphere with a very small amount of melt is present. However, it is worth noting that such an assumption is more problematic for a convecting, denser water ocean underneath an icy lithosphere.

It is likely that all four terrestrial planets have some intensity of mantle convection at present as part of their suite of processes for achieving heat release. The vigor of these convections is dependent on the temperature gradient across the mantles, which is a function of both their radial thickness and their prior cooling histories. Consequently, thinner mantles such as for Mercury and Mars will have lesser convective vigor because they have released a greater proportion of their heat through time due to relatively greater surface areas versus volumes, as compared to Venus and Earth. Therefore, we would predict that active-lid tectonics driven by mantle convection is only a possibility for Venus and the Earth. It is also worth noting that if we can trigger lithospheric failure and feed it directly into the mantle circulation, any descending lithosphere will enhance convection by materially strengthening and increasing the magnitude of thermal downwelling (Figure 7.4).

9.3.2 Density Inversion Sources

Inside a planet or satellite, a system is gravitationally more stable if more dense materials are closer to the body center than less dense materials. The classic example from the Earth is the inward vertical stacking of the least dense quartzofeldspathic crust on an ultramafic mantle on the most dense, iron-rich core (pictured in Figure 7.2). Another important example of this type of gravitationally stable stacking for icy satellites is the presence of less dense icy lithosphere on either an underlying water ocean or rocky mantle that are both more dense. Yet, not all planets and satellites have this form of gravitational stability throughout their histories. When absent, the body is gravitationally unstable, which may trigger deformation driven by the potential energy release of lowering the more dense material closer to the body center. A good example from the early Solar System of such a release of potential energy was the differentiation of mantles and cores for terrestrial bodies that was achieved by the iron metal and sulfides sinking to body centers (Section 6.2.3). This process primarily focuses on the negative buoyancy of the iron-rich materials as it is mainly about core formation.

More typically, nearer the surface of planets and satellites, we focus on cases of positive buoyancy where the upward rise of less dense materials with related "floundering" or burial of more dense material downward releases potential energy and achieves gravitational stability (Section 8.7). A smaller-scale example that is peculiar to the Earth is the formation of salt diapirs where mobile, less dense, weak salts exploit geometric irregularities in stratigraphic sequences to create vertical paths upward, displacing denser overlying sediments downward. Perhaps a more significant case with respect to lithospheric-scale deformation is the rise of hotter, less dense mantle rocks as plumes or less dense magmas within a planet or satellite.

9.3.3 Tidal Sources

If they do not spin or orbit around other bodies, planets and larger satellites tend to adopt spherical shapes achieving gravitational equilibrium (Section 8.4). When they spin, they develop an oblate spheroid shape where an equatorial diameter is greater than the polar diameter as a function of rotation rate, object size, object mass, and the material behavior(s) of the body. When a spinning body orbits around a larger body, the two bodies are gravitationally attracted to each other. This attraction further distorts body shapes, creating an ellipsoid shape due to the formation of two tidal bulges (Figure 9.3a) where the longest axis (diameter) points toward the other body and the shortest axis (diameter) is still the polar one. Ideally, a less massive body will orbit around a more massive body and have a circular orbit so that the shape of the bodies remain constant while changing orientation as a function of orbital position, which produces tides (Figure 9.3b).

If we are dealing with a less massive orbiting satellite, such as the Moon for the Earth or a satellite of Jupiter, another important effect occurs. While it is true that the tidal bulge migrates around the satellite as it orbits, this change in shape is not instantaneous because the satellite rock and/or ice actually takes time to deform. Consequently, the bulge is not exactly where it should be and as a result, the gravitational attraction of the host planet exerts a torque for the purpose of moving the actual bulge back to its ideal position (Figure 9.3c). Ultimately, this torque and the related work are eliminated in the system by locking the orbiting satellite so the tidal bulge occupies the same material points at all times, which means that the satellite takes exactly the same amount of time to complete one spin on its axis as to complete one orbit around its host. This tidally locked behavior applies to the Moon and major satellites of the gas giants in the Solar System. In the case of two bodies with similar masses, both bodies become tidally locked to each other, as with Pluto and Charon.

To this point, we are discussing gravitational and motion effects that do not generate the stresses needed to initiate active-lid tectonics. We can change that state of affairs by considering the major moons of Jupiter and Saturn, which are massive hosts compared to their satellites, and where we are changing from a "two-body system" to a "multi-body system." Having several satellites around a planet leads to the satellites having elliptical orbits because each satellite not only experiences gravitational attraction from the planet but also the other satellites (Greenberg et al., 1998). Put differently, the gravitational attraction of the other satellites changes the shape of any satellite's orbit from circular to elliptical. For example, consider Europa orbiting Jupiter with

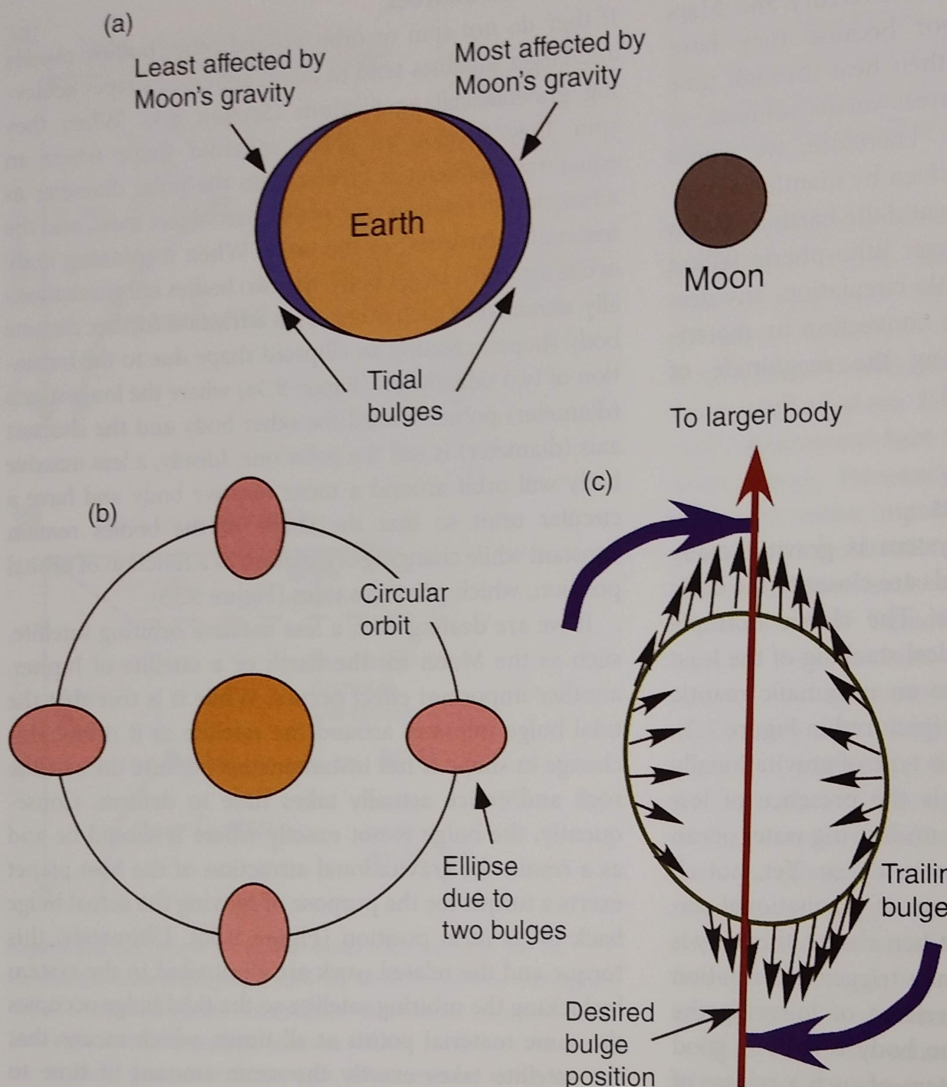

Figure 9.3 (a) Two tidal bulges created by gravitational attraction on one body by another, illustrated using gravitational attraction of the Moon on Earth's oceans because they are more responsive than the solid Earth. (b) Orientation of tidal bulges for less massive body in a circular orbit about a more massive body. (c) Torque on bulge flexing the orbiting, less massive body to re-align the actual bulge to the "instantaneous" bulge orientation.

gravitational interactions with Io and Ganymede such that its orbital eccentricity is 0.01, which while small is sufficient to generate gravitationally driven stresses that trigger stresses sufficient to cause lithospheric deformation, and by flexing the satellite generates heat (Section 6.2.4). The stresses are created by two effects: (1) tidal stress is greater when Europa is closest to Jupiter at pericenter and less when it is furthest at apocenter; and (2) while Europa's rotational speed is constant during an orbit, it should vary such that it is faster near pericenter and slower at apocenter. The first effect changes the amplitude of the tidal bulge and the second effect causes the tidal bulge to "wobble" such that the bulge is ahead of its expected position leaving pericenter and behind leaving apocenter. These variations create a "diurnal tide" that is a daily (one orbit of about 3.5 Earth days around Jupiter), and hence rapid phenomenon for Europa. As a result, stresses are created with the potential to deform the lithosphere and, just as importantly, work done flexing the satellite generates heat, creating the water-dominated ocean beneath the satellite's icy lithosphere and above its rocky interior.

The existence of an off-center bulge and a water ocean beneath the icy lithosphere introduces an important effect that adds not only to the stress sources for lithospheric deformation, but also the complexity of the possible structural geometries: **nonsynchronous rotation**. For Europa and some other icy satellites such as Enceladus around Saturn, a water ocean decouples the icy lithosphere from the rocky interior so that it can operate with a degree of mechanical independence. For Europa, this independence means that when the icy lithosphere experiences a gravitational torque attempting to pull the tidal bulge back into an ideal position, the icy lithosphere spins just a little faster than the rocky interior, creating nonsynchronous rotation (Figure 9.4a). This rotation means that a point on the surface of the lithosphere moves perpendicular to longitude and does not have a fixed position with respect to Jupiter. Further, through time, it will move onto a tidal bulge experiencing tensile stresses as it expands and off of a bulge experiencing contraction and compression (Figure 9.4b). Several lines of physical evidence support the existence of nonsynchronous rotation: (1) the crater abundance on the leading hemisphere for Europa is not greater than for the trailing hemisphere as would be expected for a fixed lithosphere; (2) Europa contains many tectonic structures that are not predicted to occur where they do if only diurnal tidal stresses exist; and (3) comparison of the change in position of structures to comparable Europan terminators from images for the *Voyager* and *Galileo* missions allow for this type of motion. As we will see, the combination of diurnal tides and nonsynchronous rotation creates rich structural suites on icy satellites such as Europa and Enceladus.

9.3.4 True Polar Wander as a Source

The existence of decoupled icy lithospheres for some satellites of the gas giants allows for another type of absolute motion of the icy lithosphere relative to the satellite center that can create lithospheric deformation: **true polar wander**. This can occur when polar ice is much thicker than equatorial ice, causing the lithosphere to move perpendicular or obliquely to latitude across the tidal bulge (axis) to compensate by relocating the thicker lithosphere at the tidal bulge. Also, major density variations in the icy lithosphere or even large impacts can trigger some true polar wander because of the relative ease of motion due to lithospheric decoupling above the ocean. Consequently, unlike nonsynchronous rotation, true polar wander is not restricted to motion perpendicular to longitude. It could in fact be perpendicular to latitude (Figure 9.4c). For example, a recent large-scale topographic analysis indicates that true polar wander may have occurred for Enceladus, repositioning which parts of the lithosphere were located at both the poles and equator (Tajaddine et al., 2017).

9.4 Structures and Tectonics for Stagnant Lids

Stagnant lids are foreign to our terrestrial experience, but they are far more common than active lids. Let's see how deformations are expressed under these conditions.

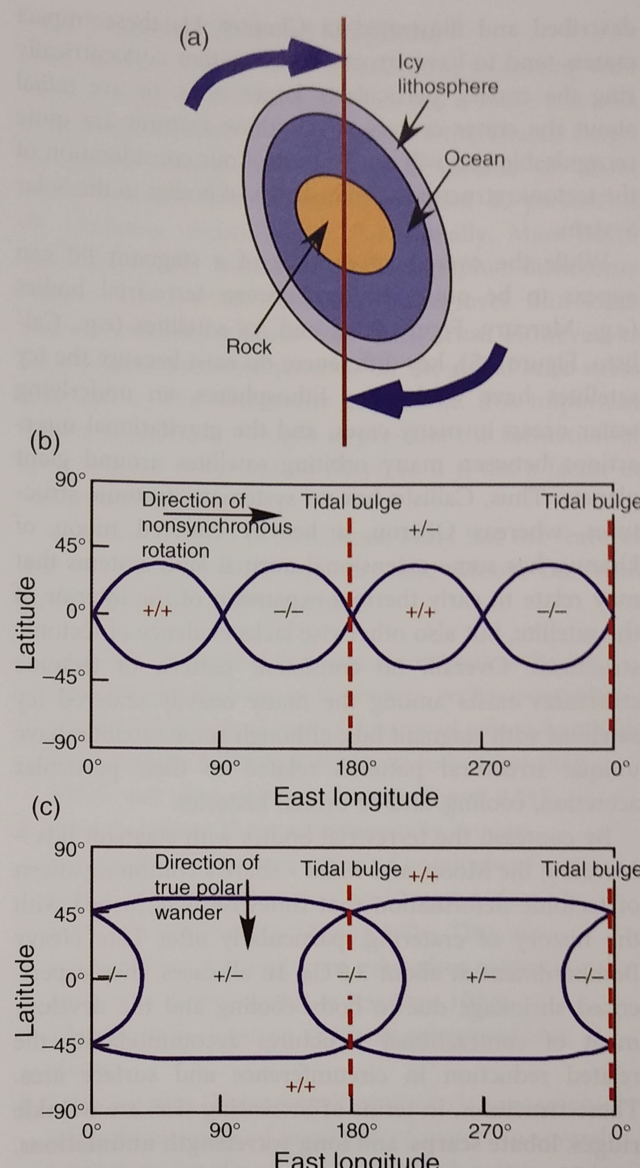

Figure 9.4 (a) Decoupling of icy lithosphere from rock interior by the intervening ocean that allows the icy lithosphere to move separately relative to the interior, creating nonsynchronous rotation. (b) Map view of deformation due to an eastward-moving nonsynchronous rotation of icy lithosphere over tidal bulges. Around the equator, it extends and contracts, leaving bulges. (c) Map view of deformation due to southward-moving true polar wander of icy lithosphere over tidal bulges, where portions extend approaching the bulges and contract moving away. Plus and minus identify surface extension and contraction; in pairs, first symbol is east–west trending and second is north–south. Modified from Collins et al. (2010).

9.4.1 Simple Stagnant Lids (Mercury, Callisto)

The signature surface appearance of a satellite or terrestrial planet that has experienced stagnant-lid tectonics is a great abundance of impact craters rather than a great abundance of tectonic structures (Figure 9.1a). As is described and illustrated in Chapter 11, these impact craters tend to have structures that either concentrically ring the craters, particularly larger ones, or are radial about the crater centers. Thus, these features are quite recognizable and will not be part of our consideration of the tectonic structures and histories of bodies in the Solar System.

While the overall appearance of a stagnant lid can appear to be quite similar between terrestrial bodies (e.g., Mercury, Figure 9.1a) and icy satellites (e.g., Callisto, Figure 9.5), key differences do exist because the icy satellites have weaker icy lithospheres, an underlying water ocean in many cases, and the gravitational interactions between many orbiting satellites around giant planets. Thus, Callisto has no systematic tectonic structures, whereas Oberon, a heavily cratered moon of Uranus, has some extensional normal fault systems that may relate to early thermal expansion of the interior of the satellite, but also otherwise lacks evidence of tectonic structures. Overall, no consistent pattern of tectonic structures exists among the many heavily cratered icy satellites with stagnant lids, although some satellites have unique structural patterns related to their particular accretion, cooling, and/or orbital histories.

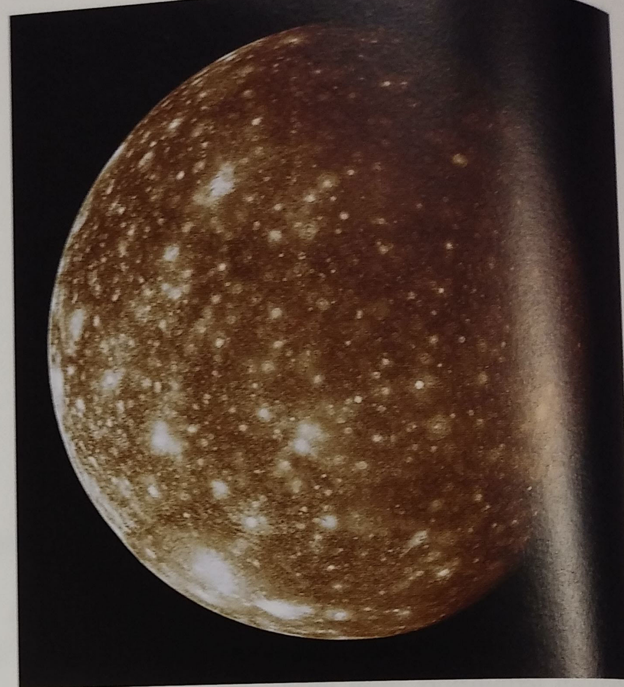

Figure 9.5 Image of Callisto showing abundant craters. NASA image.

By contrast, the terrestrial bodies with stagnant lids – Mercury, the Moon, and Mars – share a common pattern of tectonic deformation that timewise is entwined with the history of cratering, particularly after Late Heavy Bombardment at about 3.8 Ga. In all cases, they experienced shrinkage due to body cooling and the development of contractional structures accommodating the related reduction in circumference and surface area. These structures, in terms of increasing size, are **wrinkle ridges**, **lobate scarps**, and **long-wavelength undulations**. Wrinkle ridges and lobate scarps are interpreted to be fault-related folds in the hanging walls of thrusts (Figure 9.6). Wrinkle ridges on Mercury have topographic reliefs of less than 500 m and lengths of less than 100 km, whereas lobate scarps have topographic reliefs of 500–1500 m, and even up to 2000 m, with lengths that are 100 to more than 500 km. Both types of structure have asymmetric topography with relatively longer, shallower slopes that are thought to be above the underlying thrust faults. Thus, the asymmetric shape and positive topographic relief represent contractional displacement accumulation in the hanging walls above and along these thrusts at the surface of a terrestrial body. By making assumptions about the dip and shape (e.g., planar, listric, etc.) of these unexposed subsurface faults, the amount of crustal shortening achieved by individual or groups of wrinkle ridges and lobate scarps can be determined from the shapes and sizes of their topographic slopes (Figure 9.6c). Similarly, the larger undulations are treated as folds with amplitudes of 1–3 km and wavelengths of 800–1300 km, so that their shortening can be determined by comparing their wavelength to their curvilinear length, including amplitude.

Considering this cooling contractional deformation with *MESSENGER* data for Mercury (Byrne et al., 2014; Crane and Klimczak, 2017), almost 6000 contractional structures were identified and characterized in terms of size, orientation, shortening magnitude, and relative age where a tectonic structure and impact crater rim intersected. To determine the planet-scale cooling contraction, eight great-circle traces were positioned on the planet surface and the total shortening for the intersected contractional structures was calculated. This analysis determined a 7 km reduction in radius for Mercury with a related ~44 km reduction in planetary circumference. Turning to relative ages for the contractional structures and using the crater-related stratigraphy for Mercury, the oldest Pre-Tolstojan/Tolstojan craters are almost all cut by younger faults, whereas over half of the younger Mansurian craters overprint older faults (Figure 9.7). Thus, almost all preserved contractional structures postdate 3.8 Ga and many are older than 1.0 Ga, indicating that after Late Heavy Bombardment, crustal contraction was faster earlier in the history of Mercury than later. Such a result is consistent with models for thermal cooling of Mercury and other stagnant-lid tectonic bodies. They lost heat faster in the past when they were hotter because radioactive decay rates were greater, so they would

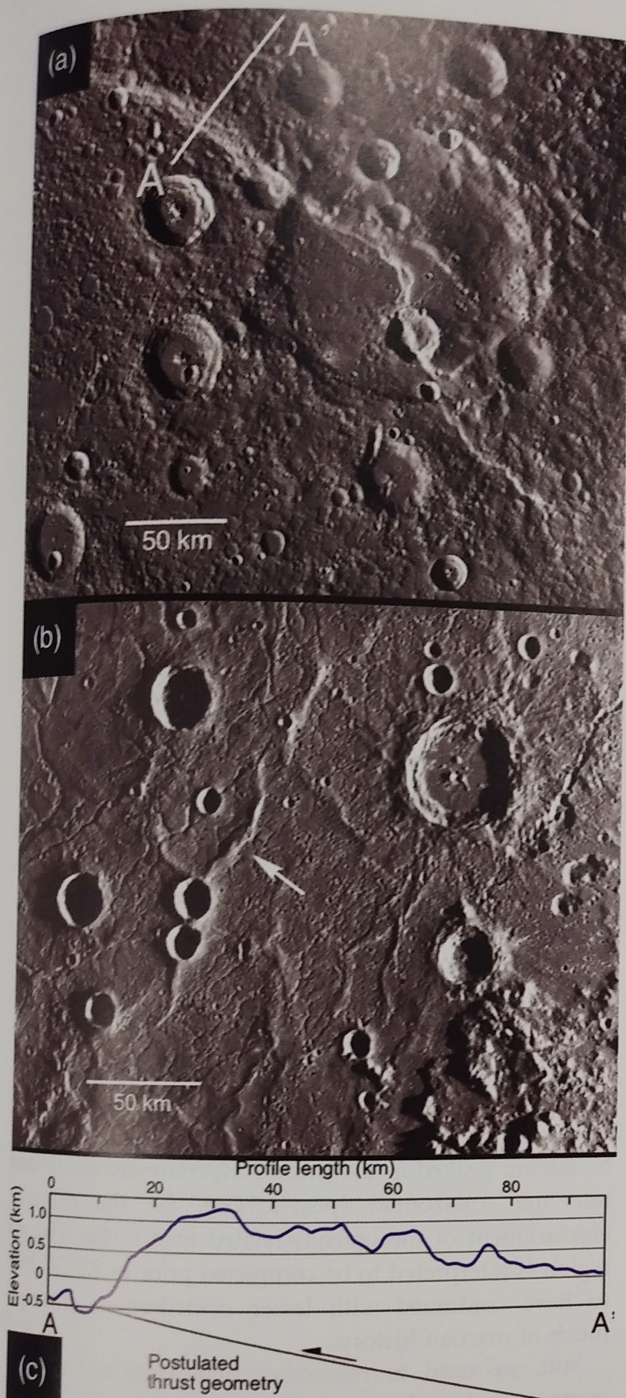

Figure 9.6 Contractional structures on Mercury. (a) Lobate scarp deforming a large crater. (b) Smaller wrinkle ridge. (c) Example of geometric assumptions for determining magnitude of crustal shortening (Byrne et al., 2014, supplemental materials). NASA *MESSENGER* images.

have contracted more then. Still, one should remember that the total shortening for Mercury due to cooling-driven contraction is about 0.3 percent, which is trivial compared to the shortening for any mountain belt on Earth.

9.4.2 A Loaded Stagnant Lid (Mars)

Mars shares a history of contraction due to cooling with Mercury and the Moon. Yet, Mars has a more complex tectonic history due to the presence of the Tharsis bulge, an igneous-related feature with a volume of about 3×10^8 km that has a footprint of about 20 percent of the planetary circumference. Additionally, Mars has a third important feature – its topographic dichotomy between the northern lowland plains over thin crust and the southern uplands over thick crust. However, as the predicted structural patterns for the global-scale stress field due to this dichotomy are absent, this important feature is generally thought to pre-date the formation of most tectonic structures on Mars, so it is not a factor in our considerations.

In terms of types of structures, Mars has the features that we have seen on Mercury and Moon, but with greater abundances (Figure 9.8):

1. Grabens: These pairs of facing extensional faults are separated by distances of kilometers, with topographic reliefs of hundreds of meters, lengths of tens to hundreds of kilometers, individual displacements of less than 100 m, and often occur as clusters (Figure 9.8a).
2. Wrinkle ridges: These asymmetrically sloping topographic ridges have reliefs of hundreds of meters, widths of tens of kilometers, and lengths of tens to hundreds of kilometers (Figure 9.8b). They are interpreted as resulting from subsurface contractional faults with displacements of less than 100 m. They typically occur on relatively uncratered lava plains.
3. Lobate scarps. These larger asymmetric topographic ridges have reliefs of hundreds of meters to several kilometers, lengths of hundreds of kilometers, and interpreted underlying thrust faults with displacements of hundreds of meters. They are more abundant in more intensely cratered regions, particularly in the southern uplands, and locally wrinkle ridges in plains continue into a lobate scarp in more intensely cratered regions.

The big difference with Mars compared to Mercury or the Moon is the arrangement of these structures on the surface of the planet (Golombek and Phillips, 2010). Many extensional grabens are arranged radially around the Tharsis uplift and many wrinkle ridges and lobate scarps are arranged concentrically. Such a geometric relationship between these structures and this major martian province favors the potential for a genetic relationship between them. As it happens, such a relationship can exist, but it derives from a stress driver that we have not previously considered: vertical lithospheric loads.

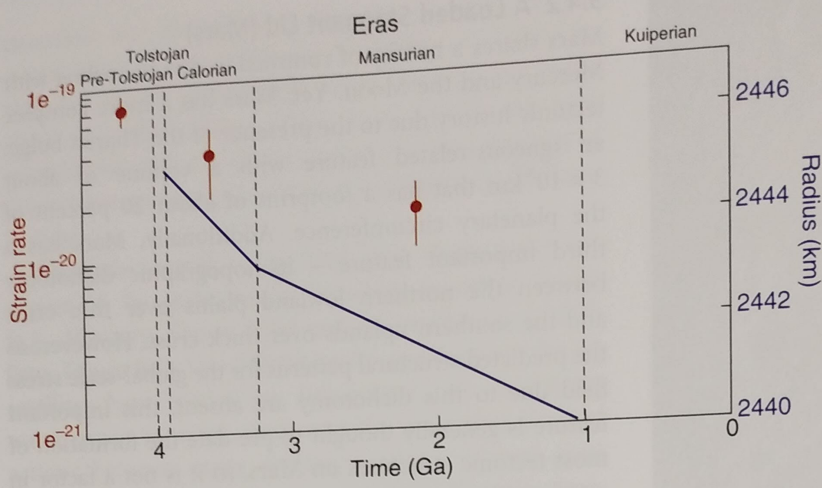

Figure 9.7 Graph showing decrease in magnitude of contraction by cooling through time for Mercury. Blue line shows change in radius with time, and red dots show average strain rates for particular times. From the right axis, one can see that the planetary radius decreased by up to 7 km. Modified from Crane and Klimczak (2017).

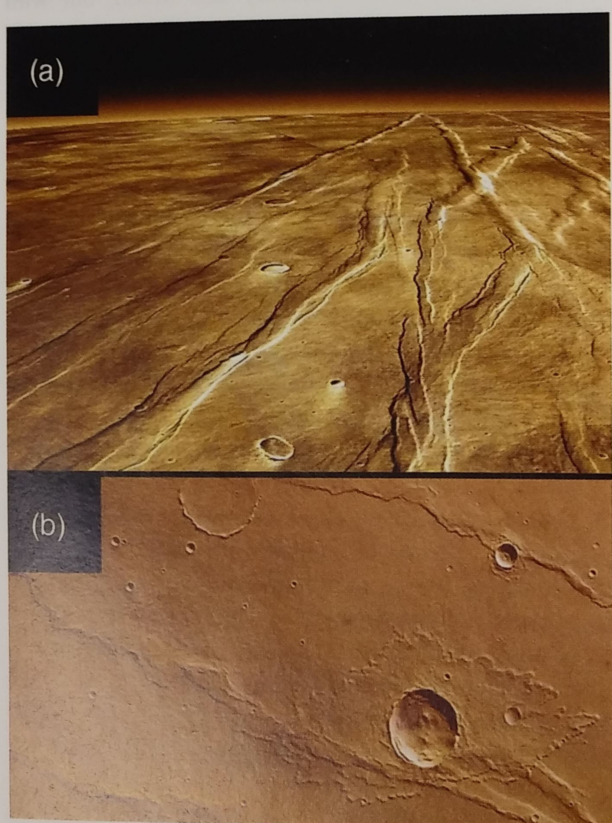

Figure 9.8 Common types of tectonic structures on Mars. (a) Complex rift system of parallel normal faults. (b) Parallel wrinkle ridges. NASA images.

The outer lithosphere can be treated as an elastic shell with flexural rigidity that means that it has a bending strength and will support loads over geologically long periods of time (Section 8.3). While this bending behavior can create suites of structures with concentric and/or radial geometries around the causative load (e.g., advancing thrust system, intruded igneous province, emplaced wedge of sedimentary rocks), these tectonic outcomes are still relatively local in character and hence not typically part of our consideration of behaviors for entire planets and satellites. Yet, given the size of Tharsis, the tectonic response of Mars to this massive load is actually planet-scale (Figure 9.9). Such a lithospheric loading creates radial horizontally directly maximum compression outward, which provides the driving stress to form the wrinkle ridges and lobate scarps that are tangential to the load geometry (Figure 9.9a). Likewise, the minimum horizontal stress is tangential to the load geometry, so that grabens can form radially. These grabens may be singular pairs of faults, many clustered pairs, which is typical, and even one of the largest grabens in the Solar System, Valles Marineris. Using the age relationships of these faults to craters and sedimentary units, structural development due to Tharsis-related loading began in the Noachian, peaked in the Early Hesperian and continued into the Amazonian (post-2.5 Ga). So, the primary emplacement of the igneous-related load in the Tharsis region is interpreted to be completed prior to 3.0 Ga, but to have continued with lesser contributions through much of martian history.

Still, we need to remember that Mars experienced contractional cooling as well. Evidence for this typical stagnant-lid behavior is the occurrence of populations of wrinkle ridges in the lava plains of the eastern martian hemisphere away from Tharsis and on the northern lowland plains, where ridge trends do not match the predicted geometries for genesis by Tharsis. Second, in regions around Tharsis, lateral-slip faults, which are near vertical faults with horizontal displacements and are rare for stagnant-lid tectonics, occur with lengths of up to a few hundred kilometers and displacements of 5–10 km (Figure 9.10) (Andrews-Hanna et al., 2008). They are unlike grabens and thrust-related folds because they have

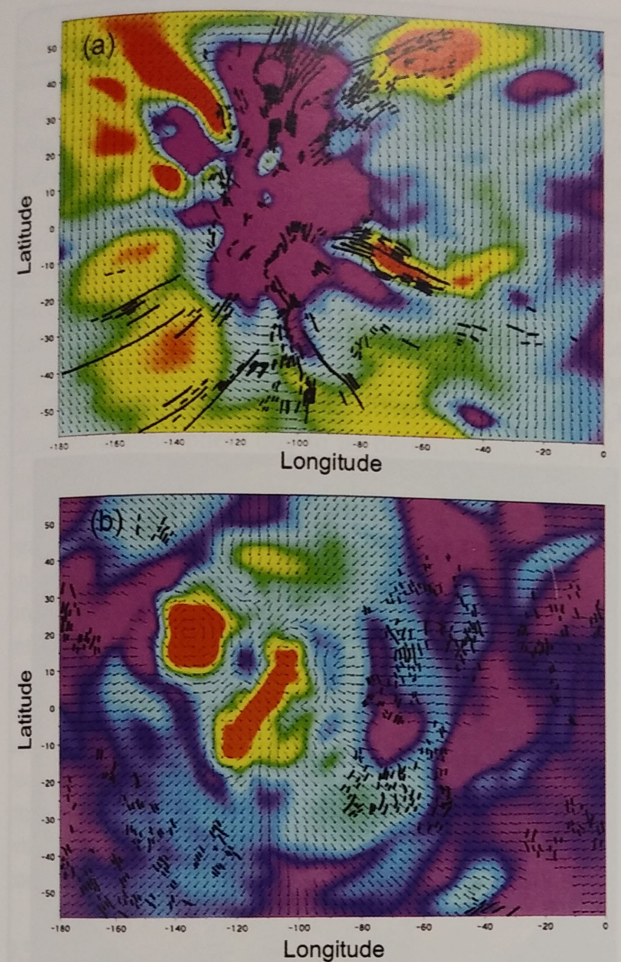

Figure 9.9 Maps showing the results of modeling the strains for flexural loading of Mars by Tharsis. (a) Major volcanoes are located in the purple region. Arrow pairs show the maximum extension directions from the load and are mostly perpendicular to the black bold traces of the major normal faults. (b) Major volcanoes are located in the red regions. Arrows show the directions of maximum contraction from the load and are mostly perpendicular to the short bold traces of wrinkle ridges. After Golombek and Phillips (2010).

both the minimum and maximum stresses trending horizontally, which does not happen with simple cooling contraction where minimum stress is typically vertical or with flexural loading. So, their occurrence implies that the stress fields created by lithospheric loading from Tharsis and cooling contraction operated at the same time for some period, such that their addition created the situation in which both the minimum and maximum stresses were horizontal. This outcome is a very important lesson: Structures may result from more than one driving stress operating simultaneously.

So, in summary, while in comparison to other bodies with stagnant lids Mars can be seen to have had more tectonic deformation for a longer period of its history, the overall deformation is still very modest, with total strains of only a few percent. Mars in this context can be seen as "active," but it was certainly not a body with an active lid as we will see.

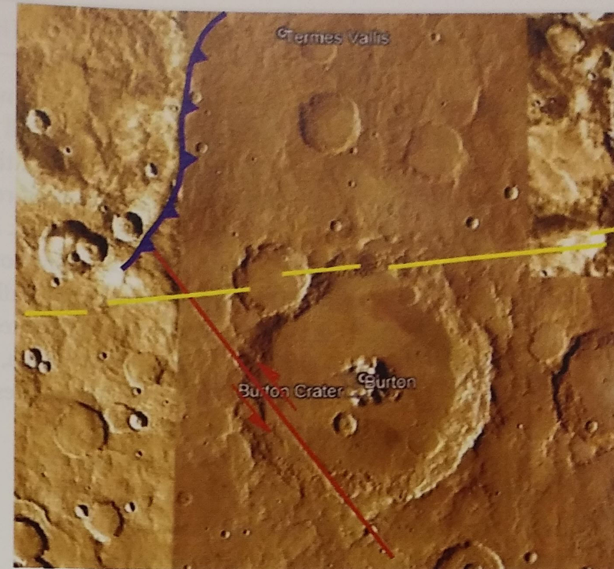

Figure 9.10 Example of evidence for a lateral-slip fault (red line) on Mars. A wrinkle ridge (blue line ornamented with triangles) and a graben system (yellow lines) are present. After Andrews-Hanna et al. (2008).

9.5 Structures and Tectonics for Active Lids

Active lids may seem synonymous with plate tectonics. As we will see, however, lithospheres (or more properly, cryospheres) can actively deform in other ways.

9.5.1 Active Lid with Plate Tectonics (Earth)

The signature active-lid tectonic system belongs to Earth and is plate tectonics. Given that a great deal has been written about plate tectonics for the Earth, we simply focus on a few observations that relate to our overall consideration of stagnant-lid versus active-lid tectonics. The cooling Earth provides sufficient energy through mantle convection to create translithospheric faults/shear zones, so that the lithosphere is a series of pieces that move from spreading centers where new lithosphere forms to subduction zones where lithosphere is returned to the mantle. Because the mantle is "self-heating" due to radioactive decay, more heat flows out of the top of the mantle and to the Earth's surface than into the bottom of the mantle from cooling of the core due to its solidification. As a result, downwelling is more important in mantle convection and is enhanced by the insertion of the colder, stronger subducting lithosphere.

BOX 9.1 THARSIS-DRIVEN TECTONIC DEFORMATION: WHEN, WHERE, AND HOW DO WE KNOW?

The formation of Tharsis as a very large igneous province flexurally loaded the martian lithosphere at a planetary scale. While this loading is elastic for small deformations (Section 8.3) and modeled elastically to predict expected strains and structures (Figure 9.9), the magnitude and duration of the Tharsis load created permanent deformation with an impressive suite of related structures. Thus, the formation of Tharsis and its related structures was not simply an elastic event. Loading yielded abundant populations of normal faults and wrinkle ridges, and we would like to document how these structures accumulated through billions of years to better understand the history of loading and, ideally, the formation of the Tharsis bulge.

An approach is to consider the geometries of all related tectonic structures around Tharsis, particularly in the western hemisphere of Mars. Using *Viking*-derived data, Anderson et al. (2001) were the first to use this approach and mapped a total population of about 24,500 structures, of which ~20,000 are normal fault systems and ~4500 are wrinkle ridges. Their analysis was superseded by the study by Bouley et al. (2018), who used data from many recent obiter missions and derivative products including a new Mars geologic map (Tanaka et al., 2014). Their mapped structures are illustrated on a Google Mars basemap in Figure 9.11. Rather than just counting numbers of faults within particular stratigraphic intervals, Bouley et al. determined the lengths of the fault traces, as a more complete proxy for the magnitude of deformation, and considered deformation intensity in terms of fault trace-length as a function of area with respect to time (Figure 9.12). Following these results, we would first determine the age of each structure by correlating this age to the youngest age of the rocks deformed by it. With these age determinations, we then define six stages of structures (Figure 9.12): Early/Mid-Noachian, Late Noachian, Early Hesperian, Late Hesperian, Early Amazonian, and Middle Amazonian to the present (refer to Figure 3.7 for the martian timescale). In terms of structural abundance (Figure 9.12), fault trace-length intensity peaked in the Early Hesperian for both radial extensional faults and concentric contractional faults (wrinkle ridges). If structure abundance equates to the magnitude of deformation, then Tharsis loading has caused extensional faulting from Early Noachian time onward, whereas contractional faulting was concentrated in Late Noachian through Hesperian time. We should also note that the rate of fault formation would have decreased markedly in the Amazonian, given the long duration of that time period (Bouley et al., 2018).

As determined by both Anderson et al. (2001) and Bouley et al. (2018), the center of igneous activity and the related development of extensional and contractional faults in Tharsis moved within the region through time (Figure 9.11). Consequently, questions remain for future researchers as to how the change in load center positions correlates with igneous eruptions and mantle circulation, and why crustal contraction related to Tharsis loading is focused in time, unlike crustal extension.

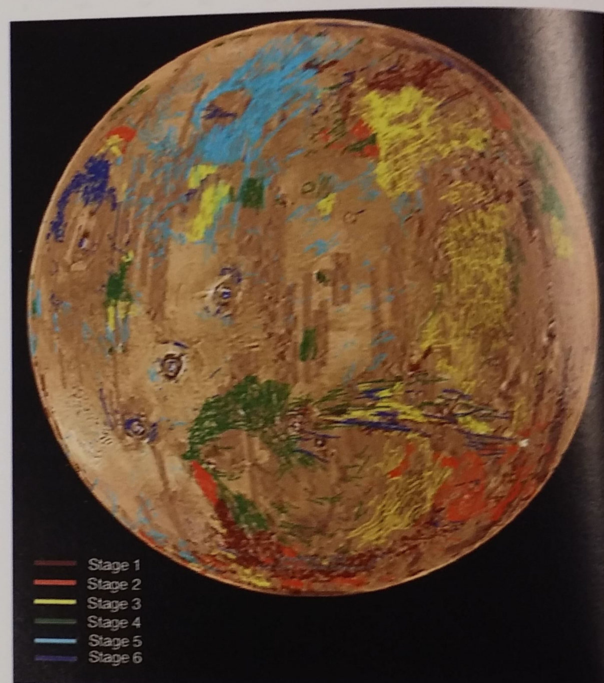

Figure 9.11 Mars paleotectonic map, centered on Tharsis, showing populations of normal (radial extensional) faults and wrinkle ridges (concentric contractional structures). Base image is from Google Mars, and fault traces are from a.KMZ file in the Supplemental Materials of Bouley et al. (2018). Colors represent the different time stages for the sequence of structure formation (periods given in Figure 9.12).

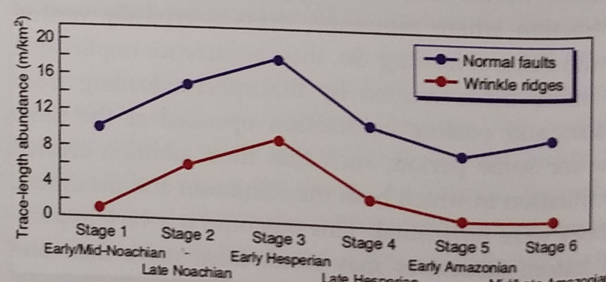

Figure 9.12 Graph of the changing abundance of fault traces for different time stages and the ages of the host units for the faults. Data are modified from Bouley et al. (2018).

A signature of plate tectonics is the importance of horizontal displacements in the lithosphere along major lateral-slip transform faults, but also at the top of subduction zones, along the major thrust faults of mountain belts and the major normal faults of extensional terranes. Individually, these faults may have up to hundreds of kilometers and collectively thousands of kilometers of horizontal displacement. While it is possible to have active-lid tectonics without these major horizontal displacements, they are a requirement of active lids with plate tectonics.

Another important aspect of active-lid tectonics for the Earth is that lithosphere is recycled and replaced. While continental lithosphere due to its buoyancy may survive on the outside of the planet for billions of years, oceanic lithosphere is typically recycled in fewer than 250 million years. Thus, even though the lithosphere has some mechanical independence from the Earth's interior due to the presence of underlying asthenosphere, it is part of the integrated heat-flow system for the planet. It assists with heat outflow at spreading centers and heat return at subduction zones. So, again, while it is possible to have active-lid tectonics without lithospheric recycling, the recycling is a requirement of plate tectonics. These distinctions between the existence of active lids with and without plate tectonics are important, as we will see when considering active icy satellites.

9.5.2 Active Lid without Plate Tectonics (Europa)

Probably the body with the greatest activity but no plate tectonics in the Solar System is Io. However, as its development is mainly the result of essentially vertical tectonics, including a daily topographic tidal range of 100 m, related to igneous-dominated rather than tectonically dominated processes, we will not consider its development.

Instead, we will consider two satellites with icy lithospheres: Europa in the Jovian system and Enceladus in the Saturnian system. Both are active bodies, but they differ in structural and tectonic development due to factors such as distance from their host planet, the number of other satellites with which they interact gravitationally, and the thickness variation of their lithospheres.

Europa is clearly a recently active if not a currently active tectonic body, given a very limited number of craters indicating an average surface age of 40–90 Ma. It is also covered by structures (Figures 3.10, 9.13). In fact, these structures have sufficient complexity to have spawned a special vocabulary exceeding 40 terms just for naming their types. If the driving stresses for deformation mainly yielded simple effects due to the diurnal

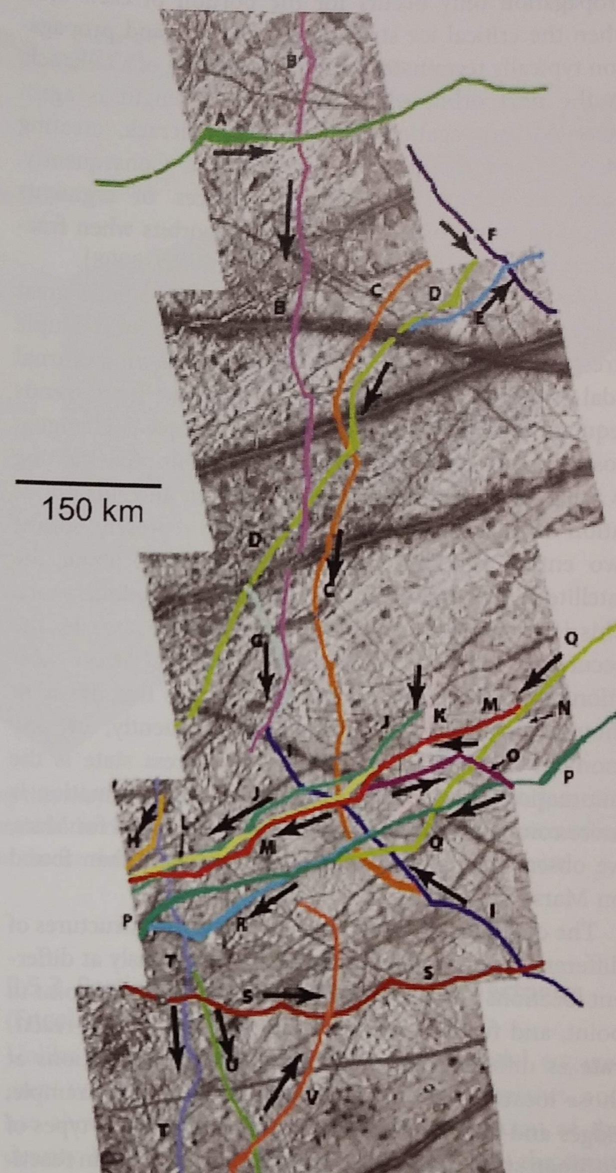

Figure 9.13 Overlapping cycloid traces in the Bright Plains area of Europa (see also Figure 3.10). Arrows are interpreted propagation directions for each trace. Modified from Groenleer and Kattenhorn (2008).

tides, the dominant structures would likely be **cycloidal traces** (Figure 9.13). They consist of multiple convex segments, where each segment has a length of about 50–200 km. A segment initiates when the diurnal tidal stress generates a sufficient tension to overcome ice strength of about 25 kPa. Segments have a direction of curvature that is a function of its propagation direction and the rotation of the stress field from the ongoing diurnal tides, a propagation velocity of about 1–3 km/h, and a depth of about 50 m up to a few hundred meters.

Propagation only occurs for the portion of each orbit when the critical ice strength is exceeded, and propagation typically terminates with the formation of a tailcrack. In the next orbit, when the critical strength is again exceeded, propagation exploits that tailcrack, creating an apex and the next curved segment. Consequently, traces in Figure 9.13 show sequences of segments recording from four to more than ten orbits when fracturing occurred (Groenleer and Kattenhorn, 2008).

The array of cycloidal traces in Figure 9.13 has a great range of trends that should not be possible for a simple stress history involving only waxing and waning diurnal tidal stresses. This assemblage of different trace trends requires that the icy lithosphere of Europa is changing position with respect to its tidal bulges. This repositioning is achieved by nonsynchronous rotation, and this population of traces has been interpreted to represent almost two entire rotations of the icy lithosphere about the satellite center that each took about 10–25 million years. This interpretation could be further complicated by the occurrence of true polar wander and local stress variations due to thermal/buoyant upwellings that are both thought to occur in Europa. Consequently, at any moment for a point on Europa, the stress state is the summation of several causes, and as that summation is more complex than, for example, we considered for Mars, we observe a more complex structural suite than found on Mars.

The complexity results from the facts that structures of different types can be occurring simultaneously at different locations because stress conditions vary from point to point, and further, structures at particular points reactivate as different structures because stress conditions at those locations also change through time. For example, ridges and **bands**, which are two very important types of Europan structures, can simply form or result from reactivation of cycloid traces. Then, they can be reactivated as lateral-slip faults or even reverse faults. Ridges are the most common structures on Europa (e.g., Figure 3.11). They can occur singly, or commonly as double ridges or ridge complexes, where this increasing geometric complexity is also thought to be a developmental sequence. Consequently, they record the complexity of a stress field that represents several drivers and is changing every orbit (3.55 Earth days). For example, the Bright Plains region records at least two complete lithospheric rotations with respect to the satellite center due to nonsynchronous rotation, while experiencing at least one billion diurnal tidal stress cycles (Figure 3.11) (Kattenhorn, 2002). These ridges represent material accumulation from the lithospheric interior onto the Europan surface, but their cause is not well understood. The material may derive from reactivation of the ridges during diurnal tidal events as faults with lateral slip,

Figure 9.14 Example of band structure on Europa. The band is a location where lithospheric dilation occurred and new icy lithosphere was added at the surface (Collins, 2010). NASA image.

if that slip exceeds 10 cm, generating sufficient heat to weaken and even melt ice, and forming material that rises to the surface. Alternately, some or all of the material may come out of the lithosphere from where a ridge fracture connects to upwelling diapiric ice or even an intruding water "magma" from below.

As common as ridges are on Europa, one can argue that bands are more important in terms of their tectonic implications (Figure 9.14). Bands are up to 30 km wide and hundreds of kilometers long, with a central trough, matching hummocky textural zones across the trough, boundaries that may include narrow parallel ridges and troughs representing normal faults, and most importantly older structures that fit back together when the band is removed. Consequently, bands are dominantly dilational structures that are places where younger lithosphere was inserted frequently as weak ice or water that froze to preserve the structural opening. Given that their widths can be up to tens of kilometers and that locally they represent 40 percent of the satellite's surface area, they indicate that Europa has experienced significant additions of icy lithosphere to its surface.

Such major additions immediately create a problem because as Europa is not an expanding body, some process or processes must shorten and/or remove lithosphere from the satellite surface. Large folds with wavelengths of about 25 km but modest amplitudes occur, but they do not represent nearly enough shortening to match the dilation recorded by bands. Similarly, thrust faults and reverse faults that reactivated other structures occur, but their effects are quite modest and insufficient. Recently, another process has been proposed to remove lithosphere from the surface, which is **subsumption** with subsumption bands

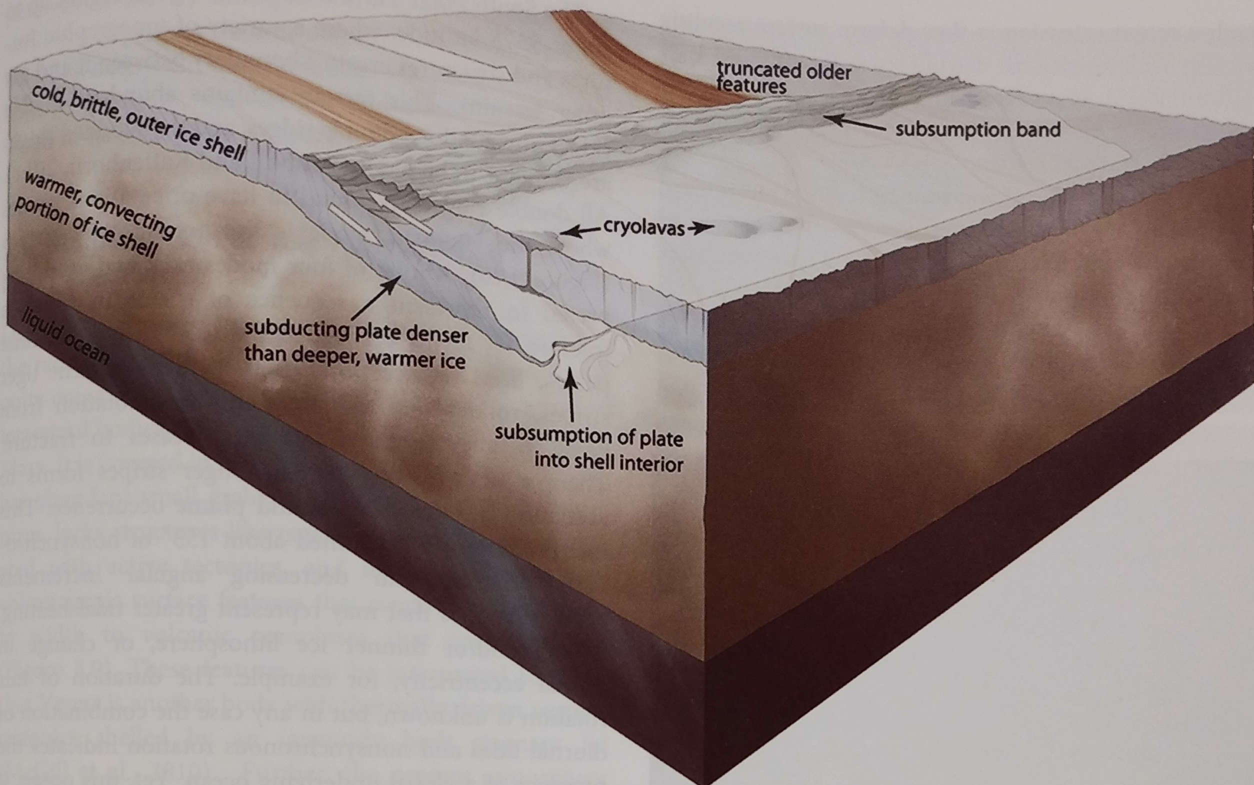

Figure 9.15 Conceptual block diagram of the process of subsumption that recycles brittle, icy lithosphere into the underlying ductile lithosphere, with creation of cryolavas that create volcanogenic landforms in the overriding brittle lithosphere. Reprinted by permission from Springer Nature: Nature Geoscience, Evidence for subduction in the ice shell of Europa, Simon A. Kattenhorn and Louise M. Prockter, Copyright (2014).

and cyrolava bodies (Figure 9.15) (Kattenhorn and Prockter, 2014). Subsumption bands contain elongate hummocks oriented subparallel to the margins, smooth regions with pits, and margin-parallel linear features; they lack central troughs and bilateral symmetry of structures within the bands, and have somewhat elevated relief as compared to adjacent regions. Most importantly, they juxtapose regions with different features that do not match across them. Given that the bands lack the relief and structure complexity to account for "missing lithosphere," this lithosphere is proposed to return by subsumption into the lithosphere. Essentially, the outer, cold, brittle lithosphere is returned, warmed and converted to either ductile lithosphere that remains in the lithosphere or provides melts that rise to form cyrolava bodies in the overriding lithosphere. Given this proposed "pairing" of bands with lithospheric addition and subsumption bands with lithospheric removal, Europan tectonics would bear kinematic similarities to plate tectonics. The key difference of this proposed system is that the addition and subtraction of lithosphere would work entirely within the lithosphere of Europa, whereas plate tectonics on Earth involve the lithosphere and the entire underlying mantle.

9.5.3 Partially Active Lid without Plate Tectonics (Enceladus)

Unlike Europa, Enceladus only has major tidal engagement with one other satellite around its host planet, and has about 1/216th of the volume and 53 percent of the density. So, Enceladus has not experienced all of the structural complexity of Europa, but the effects of diurnal tides, nonsynchronous rotation, and true polar wandering have structurally marked the surface of this satellite. Further, Enceladus is currently active – plumes of vapor and ice crystals were observed escaping from linear features ("**tiger stripes**") in its South Polar Terrain by *Cassini* (Figure 9.16).

Perhaps the easiest way to recognize the difference in tectonic histories between Europa and Enceladus is that whereas Europa has a complex array of structures across its entire surface, Enceladus has four quite different terrains. They range from a cratered terrain with crater abundances indicating a mean maximum surface age of a few billion years, to the South Polar Terrain that is devoid of craters, so that it is very young (Figure 9.17). The cratered terrain does contain troughs, pit chains, and merged pit chains that are parallel and indicate at least modest recent extension as they deform surface regolith, possibly with a tensional driving stress (Nahm and Kattenhorn, 2015). However, their occurrence does not disturb the determination of an ancient maximum age for the heavily cratered terrain.

The leading (western) and trailing (eastern) tectonized terrains contain more and a greater variety of structures than the cratered terrain (Figure 9.17). These structures include bands, **chasma**, ridges, scarps, and troughs with and without pits. The majority of these structures have been recently interpreted to result from extension without involving lithospheric surface additions, unlike Europa.

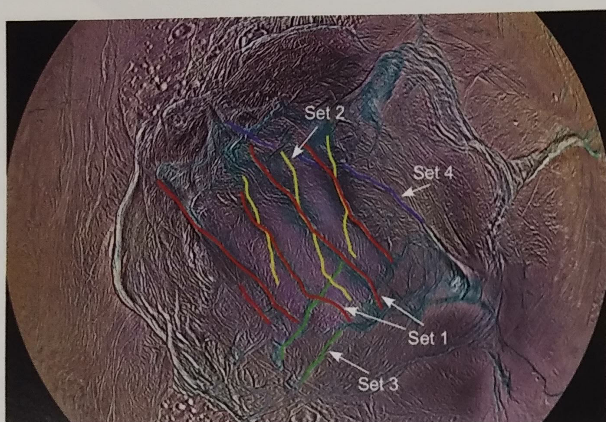

Figure 9.16 "Tiger stripe" sets of different age in the South Polar Terrain of Enceladus. By implication, the South Polar Terrain has not experienced any significant true polar wander during the development of this structural sequence. Relative age information from Patthoff and Kattenhorn (2011).

The South Polar Terrain covers that polar region up to about 55 °S latitude, where a variety of topographic features and structures create a boundary between it and the other terrains. This terrain contains abundant double ridges and subdued double ridges, and the subdued ridges are thought to be older (Patthoff and Kattenhorn, 2011). All double ridges are found to have orientations modes where the youngest mode is the present tiger stripes (Figure 9.16). A total of four modes exist and are interpreted to represent a sequence of events in which a fracture set forms parallel to the tidal bulges. As time passes, that fracture population, with its ancient tiger stripes, rotates due to nonsynchronous rotation from being parallel to the bulges and ceases to fracture. Then, a new fracture set with tiger stripes forms to accommodate deformation and plume occurrence. This interpretation has identified about 153° of nonsynchronous rotation with decreasing angular increments between modes that may represent greater tidal heating, weaker and/or thinner ice lithosphere, or change in orbital eccentricity, for example. The duration of this rotation is unknown, but in any case the combination of diurnal tides and nonsynchronous rotation indicates the presence of a global underlying ocean. Yet, this ocean, if present under all of Enceladus, has not enabled Enceladus to be tectonically active everywhere and eliminate the cratered terrains. In summary, while Enceladus has one terrain, the Southern Polar Terrain, that is possibly even more active than any location on Europa, it does not have evidence for body-scale lithospheric recycling or even satellite-wide tectonic resurfacing. Consequently, the

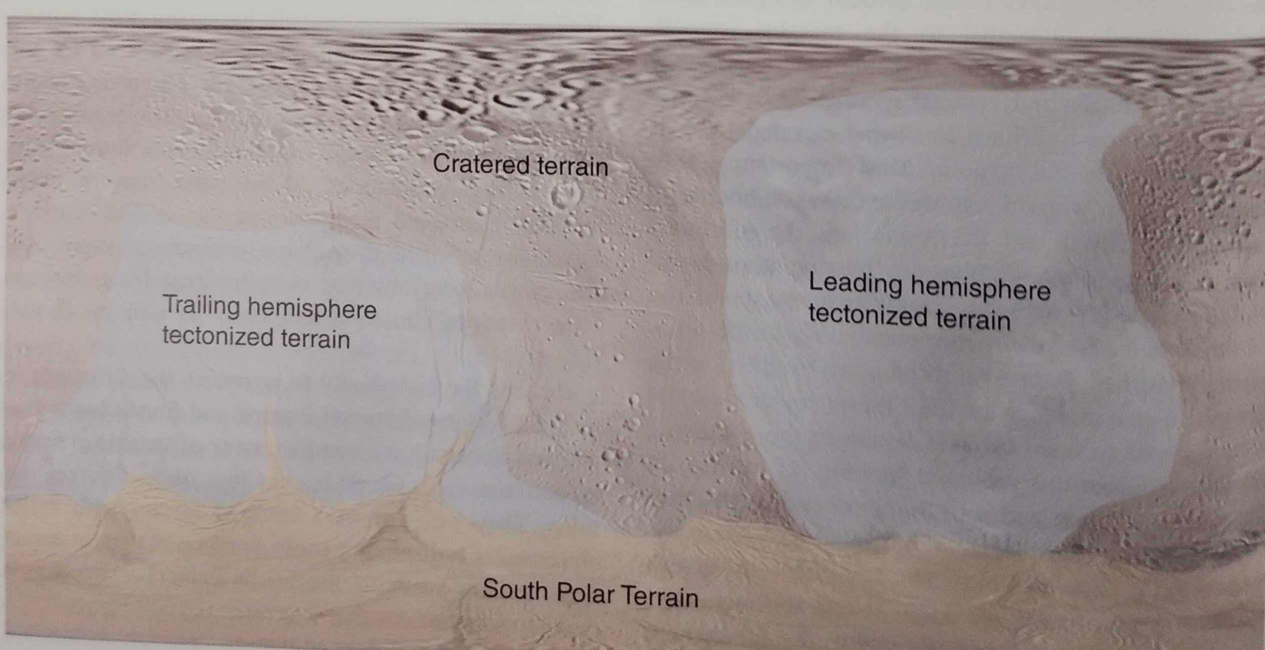

Figure 9.17 Surface topographic map of Enceladus showing the four topographic/geologic terrains.

strength of the icy lithosphere for Enceladus has been sufficient to prevent tectonic deformation driven by diurnal tides, nonsynchronous rotation, true polar wandering, density inversion, convection, and other causes over much of its surface, as compared to Europa.

9.6 Stagnant Lid Possibly Active in the Past? (Venus)

Despite having seen through the clouds of Venus using the radar data of the *Magellan* mission, the planet is still quite enigmatic. Venus has clear similarities to the other terrestrial bodies with stagnant lids, such as Mercury and Mars. It is covered in basalt, has abundant wrinkle ridges, has abundant small grabens and linear extensional fractures, lacks structures like major strike-slip faults associated with active tectonics, and has an abundance of volcanogenic surface features that range from only 1 km in width to volcanic complexes that span 1500 km (Figure 3.9). These features can be interpreted to mean that Venus is another body with thermally driven vertical tectonics shelled by an igneously built stagnant lid (McGill et al., 2010) . Further, the present atmosphere and very hot surface of Venus lack water, which implies that the current lithosphere of Venus is quite dry compared to Earth, and hence strong, which is appropriate for a stagnant lid.

Yet, Venus in terms of size and mass is very similar to Earth, the home of plate tectonics. Further, Venus has a number of unique features that are absent on Mercury, the Moon, or Mars:

1. Volcanic rises: About ten of these features occur on Venus with volumes of 10^4–10^6 km^3 and diameters of 1400–2500 km that overlie positive gravitational anomalies, which are consistent with active underlying mantle plumes.
2. Coronae (Figure 9.18a): These circular features with diameters of 50–500 km may have raised or depressed centers. They are too small and in many cases too close together to be plume-related volcanogenic features. They are commonly associated with significant volcanic flows that were typically deposited prior to concentric topographic rims that are commonly found around coronae.
3. Chasmata (Figure 9.18a): Venus has five large, complex normal fault systems with lengths of thousands of kilometers and reliefs of up to 7 km, along with a number of other, somewhat smaller systems that are preferentially located in equatorial highland regions.
4. Tesserae (Figure 9.18b): These terrains are mostly located in the crustal plateaus that topographically compose about 10 percent of the planet surface, although a few **tesserae** occur in the abundant plains of Venus. They are commonly overlapped by the adjacent terrains so that the tesserae are the oldest features. Further, they are structurally complex with sinuous topographic antiforms dissected by one or more sets of grabens and fractures.
5. A limited population of large craters: Venus has fewer than 1000 impact craters, which are all larger than 2 km in diameter because the venusian atmosphere destroys smaller possible impactors. This population is randomly distributed across the planet surface and analysis shows that their presence means that, on average, the present surface of Venus is less than one billion years old, so the surface is young compared to other terrestrial bodies with stagnant lids. Further, the planet may have been completely repaved with igneous rocks about one billion years ago.

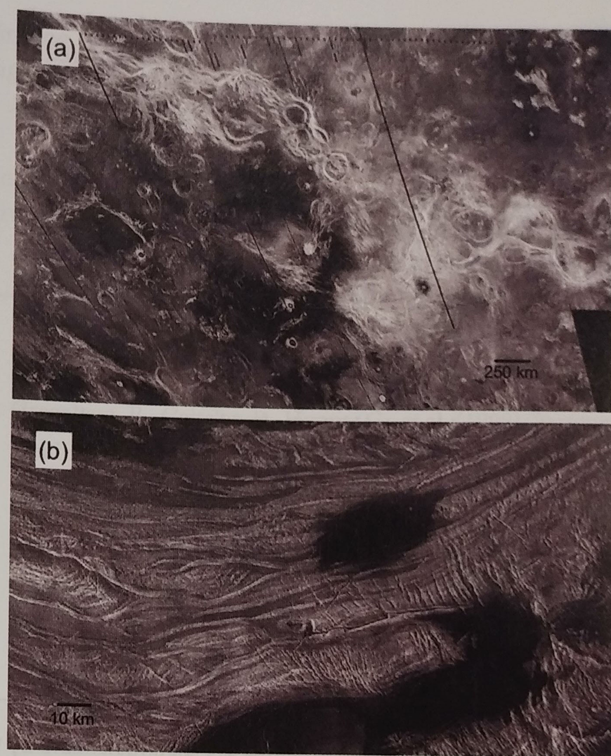

Figure 9.18 Structural features on Venus. (a) Coronae (circular structures) and chasmata (complex white linear traces from the upper left to middle right of the image). Note the scale and hence large sizes of these structures. (b) Tesserae, showing broad ridges with open folds cut by north-northwest-trending grabens. NASA *Magellan* radar images.

Still, the occurrence of volcanic rises, coronae, and chasmata would be consistent with stagnant-lid behavior, if Venus is considered to still be thermally active internally, which is appropriate for a planet that is similar in size, mass, and composition to the Earth. Where the applicability of the stagnant-lid model becomes more uncertain is when considering the tesserae, the relatively young overall age of the venusian surface as compared to other terrestrial bodies with stagnant lids, and, surprisingly, both the existence of the stagnant lid and the lack of present-day water.

The Earth loses about 70 percent of its heat at spreading centers and subduction zones while constantly replenishing surface liquids and gases from mantle volatile escape. By comparison, Venus lacks such an efficient means for releasing mantle heat or mantle volatiles. Thus, heat could be accruing beneath the present venusian lithosphere that could trigger another surface repaving event by igneous flows that would again leave isolated tesserae and result from thermally driven vertical tectonics without the need for active tectonics. Alternately, it is possible that this trapping of heat triggers a phase transition in which the lithosphere is not a distinct layer but rather compositionally continuous with the underlying mantle, allowing whole-mantle circulation to entrain the lithosphere as a part of an actively convecting system in which active tectonics temporarily operates and resurfaces the planet. Further, this possibility could have been more likely in the past because the present deuterium/hydrogen ratios for Venus indicate that it likely had about 100 times more water than it presently has. The past presence of water would have favored a weaker lithosphere and a more mobile mantle that would have supported active tectonics driven by mantle convection. Still, Venus is an enigmatic planet: It lacks erosion so a long-term complex history is preserved on its surface; it provides little data about rock compositions and ages as a function of terrains, structures, and volcanogenic features; it lacks geophysical data about its interior; and it remains shrouded in clouds.

Summary

Terrestrial planets and icy satellites are distinguishable by whether they function or functioned as stagnant- or active-lid bodies. This choice of behavior is driven by whether stress-generating agents such as mantle convection, diurnal tides, or nonsynchronous rotation are able to overcome the strength of the exterior shell (lithosphere) to trigger active-lid tectonics. If strength prevails, stagnant-lid behavior occurs. In that case, the planet or satellite is typically intensely ornamented by craters with radial and concentric structures, plus wrinkle ridges and lobate scarps that accommodate the very modest shrinkage of particularly the terrestrial bodies such as Mercury. This deformation pattern is enhanced when planetary-scale lithospheric loading, such as for Tharsis on Mars, or continuing active mantle heat circulation, as for Venus, occurs. In these cases, structures such as wrinkle ridges and graben fault systems are more abundant, with distributions that relate to the lithosphere load or the history of lithospheric responses to continuing mantle convection and plumes. Yet, when the driving stress prevails, active-lid tectonics enhances the structural complexity on the body surface. For example, Europa has a complex array of structures reflecting the interaction of diurnal tides, nonsynchronous rotation, and true polar wander in both space and time around the satellite, and a very limited population of young impact craters. Alternately, the Earth has some ancient preserved continental regions that lack craters due to complex geologic histories and an active atmosphere, but more importantly returns more than about 70 percent of its lithosphere into the interior every 250 million years as a function of convection-driven plate tectonics. Even where only partially active, the structure complexity increases greatly, as with the tiger stripes and related structures in the South Polar Terrain of Enceladus. Finally, the temporary occurrence of active-lid tectonics in the past might even explain the potentially episodic replacement of the complex geologic surface of Venus.

Review Questions

1. Considering terrestrial planets and satellites with radii greater than 200 km, are surfaces with stagnant-lid or active-lid tectonics more abundant? Why do you believe that one behavior has been more abundant than the other?
2. Why is it reasonable to say: "From a material perspective, an icy lithosphere is more likely to show evidence for active-lid tectonics than a rocky lithosphere."

3. Contrast the roles of thermal and tidal sources as driving stresses for triggering active-lid tectonics.
4. What are the similarities and differences between stagnant-lid surfaces for icy satellites and rocky planets?
5. Why is Europa interpreted to be a very tectonically active icy satellite, whereas Enceladus is a selectively active satellite?
6. Develop two lists: (a) evidence favoring Venus having always been a stagnant-lid body; and (b) evidence favoring Venus having one or more episodes of active-lid behavior in its past and/or future. Which explanation do you favor and why?

SUGGESTION FOR FURTHER READING

Watters, T. R., and Schultz, R. A., eds. (2010) *Planetary Tectonics*. Cambridge: Cambridge University Press. Chapter 3 presents information about the structural geology and tectonics of Venus, whereas Chapter 5 does the same for Mars, and Chapter 7 considers the icy satellites. Chapter 9 considers the strength and deformation of lithospheres.

REFERENCES

Anderson, R. C., Dohm, J. M., Golembek, M. P., et al. (2001) Primary centers and secondary concentrations of tectonic activity through time in the western hemisphere of Mars. *Journal of Geophysical Research*, **106**(E9), 20563–20585.

Andrews-Hanna, J. C., Zuber, M. T., and Huack, S. A. (2008) Strike-slip faults on Mars: observations and implications for global tectonics and dynamics. *Journal of Geophysical Research*, **113**. DOI: 10.1029/2007JE002980.

Boettcher, M. S., Hirth, G., and Evans, B. (2007) Olivine friction at the base of oceanic seismogenic zones. *Journal of Geophysical Research: Atmospheres*, **112**, 1205–1218.

Bouley, S., Baratoux, D., Paulien, N., et al. (2018) The revised tectonic history of Tharsis. *Earth and Planetary Science Letters*, **488**, 126–133.

Byrne, P. K., Klimczak, C., Sengor, A. M. C., et al. (2014) Mercury's global contraction much greater than earlier estimates. *Nature Geoscience*, **7**, 301–307.

Collins, G. C., McKinnon, W. B., Moore, J. M., et al. (2010) Tectonics of the outer planet satellites. In *Planetary Tectonics*, eds. Watters, T. M., and Schultz, R. A. Cambridge: Cambridge University Press, pp. 264–350.

Crane, K. T., and Klimczak, C. (2017) Timing and rate of global contraction on Mercury. *Geophysical Research Letters*, **44**, 3082–3089.

Golombek, M. P., and Phillips, R. J. (2010) Mars tectonics. In *Planetary Tectonics*, eds. Watters, T. M., and Schultz, R. A. Cambridge: Cambridge University Press, pp. 183–232.

Greenberg, R., Geissler, P., Hoppa, G., et al. (1998) Tectonic processes on Europa: tidal stresses, mechanical response, and visible features. *Icarus*, **135**, 64–78.

Groenleer, J. M., and Kattenhorn, S. A. (2008) Cycloid crack sequences on Europa: relationship to stress history and constraints on growth mechanics based on cusp angles. *Icarus*, **193**, 158–181.

Hansen, L. N., Conrad, C. P., Boneh, Y., et al. (2016) Viscous anisotropy of textured olivine aggregates: 2. Micromechanical model. *Journal of Geophysical Research: Solid Earth*, **121**. DOI: 10.1002/2016JB013240.

Kattenhorn, S. A. (2002) Nonsynchronous rotation evidence and fracture history in the Bright Plains region, Europa. *Icarus*, **157**, 490–506.

Kattenhorn, S. A., and Prockter, L. M. (2014) Evidence for subduction in the ice shell of Europa. *Nature Geoscience*, **7**, 762–767.

McGill, G. E., Stofan, E. R., and Smrekar, S. E. (2010) Venus tectonics. In *Planetary Tectonics*, eds. Watters, T. M., and Schultz, R. A. Cambridge: Cambridge University Press, pp. 81–120.

Nahm, A. L., and Kattenhorn, S. A. (2015) A unified nomenclature for tectonic structures on the surface of Enceladus: implications for Enceladus's tectonics and ice shell. *Icarus*, **258**, 67–81.

O'Neill, C., Jellinek, A. M., and Lenardic, A. (2007) Conditions for the onset of plate tectonics on terrestrial planets and moons. *Earth and Planetary Science Letters*, **261**, 20–32.

Patthoff, D. A., and Kattenhorn, S. A. (2011) A fracture history on Enceladus provides evidence for a global ocean. *Geophysical Research Letters*, **38**, L18201. DOI: 10.1029/2011GL048387.

Tajaddine, R., Soderlund, K. M., Thomas, P. C., et al. (2017) True polar wander of Enceladus from topographic data. *Icarus*, **295**, 46–60.

Tananka, K. L., Skinner, J. A., Dohm, J. M., et al. (2014) Geologic map of Mars. US Geological Survey Scientific Investigations Map 3292.

Weller, M. B., and Lenardic, A. (2012) Hysteresis in mantle convection: plate tectonic systems. *Geophysical Research Letters*, **39**. DOI: 10.1029/2012GL051232.